Bulletin of the JSME
Vol.6, No.3, 2019
Mechanical Engineering Journal

Application of DIC to deformation measurement around damages in CFRP cross-ply laminates

M.J. Mohammad FIKRY*, Shinji OGIHARA* and Vladimir Vinogradov**
*Department of Mechanical Engineering, Tokyo University of Science
2641 Yamazaki, Noda-shi, Chiba-ken, Japan
E-mail: writetofikry@yahoo.com
**School of Engineering, Newcastle University
Newcastle upon Tyne, NE1 7RU, UK

Received: 28 December 2018; Revised: 21 February 2019; Accepted: 27 February 2019

Abstract
Digital Image Correlation (DIC) is a non-contact method to analyse the deformation of materials that can measure displacement or strain behaviour during tensile loading. In this study, DIC is used to measure the deformation of cross-ply carbon fibre reinforced plastics (CFRP) laminates and for the detection of damages in them. The objective of this study is to measure the deformation around the damages in cross-ply CFRP laminates by using the DIC system from both width and thickness directions. For this purpose, thick CFRP $[0_4/90_{24}]_s$ and thinner $[0/90_6]_s$ laminates were tested. In cross-ply laminates, usually a straight transverse crack will initially occur in 90 degree ply followed by the following damages such as delamination, fiber fracture, and etc. To start, straight transverse cracks are induced in the laminates by using an artificial crack method. Then, X-ray radiography is used to detect the location of the straight cracks in order to be used for DIC observation to examine the strain distribution around the existed cracks. The DIC observation from the surface of the laminate around the cracks area clearly showed how strain is distributed from one crack to another adjacent crack. From the result, secondary mode damages of matrix cracking such as oblique and curved cracks can also be observed and are being discussed in this paper.

Keywords : DIC, Cross-ply laminates, Damages, Deformation, Matrix cracks, Secondary mode damages

1. Introduction

Carbon fiber reinforced plastics (CFRP) laminates are increasingly utilized in the aeronautical and construction industries for their low weight, high strength, and high stiffness properties. Fiber reinforced laminated composites including CFRP exhibit various competing damage modes such as matrix cracks, delamination, fiber breakage, and etc. (Jalalvand et al., 2014). Transverse matrix cracks in cross-ply laminates have been studied vigorously back in the late 1970s until now. The initial cracking in cross-ply laminates was investigated by Parvizi et al. (1978) where they examined the formation and growth of cracks in transverse plies of cross-ply laminates of glass fiber reinforced plastics under axial tension. When cracks formed under constraint, they started at the free edges and propagated inwards with increasing load. The constrained cracking behavior was confirmed by several subsequent studies including that by Boniface et al. (1997) for CFRP cross-ply laminates; where they investigated initiation of cracking by introducing notches in the transverse plies.

Study on transverse cracking was developed further in later studies (Han et al., 1988; Lim et al., 1989; Xia et al., 1993; Zhang et al., 1992; Praveen et al., 1998; Hosoi et al., 2010). These works considered stress transfer at the 0/90 interface and evaluated the energy release rate of the cracks to predict crack density in the transverse plies. With such approaches, the first cracking strain is estimated by setting the crack spacing to infinity. However, such estimate is only applicable for cracks that are fully developed along the ply thickness and propagate in the width direction of the laminate. Hosoi et al. (2010) reported that partially developed cracks formed on free edges that may not grow at a given

Paper No.19-00003
J-STAGE Advance Publication date: 7 March, 2019
[DOI: 10.1299/mej.19-00003]

applied stress could grow under cyclic application of the stress. Other than experimental studies, there are also a number of analytical studies focused on transverse matrix cracks and its effect on the mechanical properties degradation of the laminates. For example, in variational analysis, Vinogradov et al. (2010) extended Hashin (1985)'s who constructed an admissible stress field to determine the stiffness reduction and stresses on the basis of the principle of minimum complementary energy for cross-ply laminates to angle-ply laminates of type $[\theta_m/\varphi_n]_s$ containing intralaminar cracks in the middle laminae.

Delamination is reported as one of the damage in secondary mode damages in the laminates (Boniface et al., 1997; Lim et al., 1989; Jalalvand et al., 2014; Hu et al., 1993). Delamination occurring in the laminates is mostly explained by the stress concentration around the transverse crack tip and also the high value of strain energy release rate (Ogihara et al., 1995). Further transverse cracking and delamination initiating from the tips of existing transverse cracks are known as two competing damage mechanisms (Jalalvand et al., 2014). Different mathematical approaches such as variational (Hashin et al., 1985; Vinogradov et al., 2010, 2015), shear-lag (Boniface et al., 1997; Xia et al., 1993) and Finite Element Analysis (FEA) (Jalalvand et al., 2014) are also used for calculating the energy release rates; all of which may be used in comparing the energy release rates to predict the dominant damage mode.

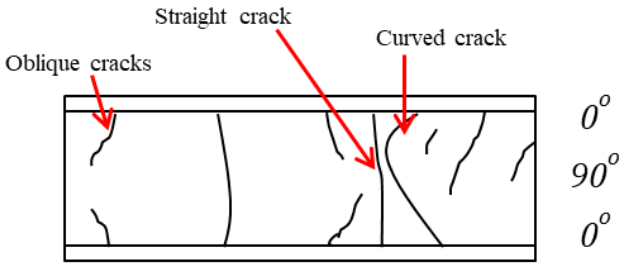

Fig. 1 Schematic of the matrix crack pattern in CFRP $[0_4/90_{24}]_s$ laminate.

Besides delamination, there are other types of cracks in secondary mode damages such as oblique and curved transverse cracks close to the straight cracks with no delamination (Jalalvand et al., 2014). Damages in this mode are shown schematically in Figure 1. Oblique crack in off-axis plies is another kind of damage in secondary mode damages which always occurs near to the straight transverse cracks while curved cracks usually form from two oblique cracks extended from the ply interface. Most of the analytical and experimental studies are focused on straight transverse cracks that fully propagates in the 90 degree ply and delamination induced by transverse cracks. Therefore, we believe that oblique and curved cracks have not yet been investigated in detail. There are few works related to this study including works done by Groves et al. (1987) and Hu et al. (1993). Hu et al. (1993) used a variational approach to find the distribution of maximum principal stress around the normal crack tips and showed that at high crack densities, the point with maximum first principal stress moves significantly away from the tips of the straight transverse cracks. While Groves et al. (1987) used FEA for the stress distribution that clearly indicated that the maximum first principal stress stays at or very close to the tips of the straight transverse cracks if linear elastic material properties are applied.

However, experimental study on the deformation measurement around the damages including transverse matrix cracking on CFRP laminates are not yet developed due to the limitation of measurement devices. Traditionally, strain gages have been used to measure the tensile strain to determine the mechanical properties of the materials such as Young's modulus, tensile strength, and Poisson's ratio. The selection of strain gages is based upon the type of material, displacement range and temperature involved during a particular test. Strain gages can only measure the average strain within the gage length and produces no information on the strain distribution in the measurement area. During tensile loading, deformation localization occurs and causes strain distribution to be non-uniform.

There are some full-field strain measurement methods that have been used in measuring the strain deformation of the composites such as digital image correlation (DIC), moiré and speckle interferometric. An application of moiré technique in shear deformation of CFRP laminated had been reported by Wang Q. et al. (2019) where the interlaminar shear behavior of a $[\pm 45°]_{4s}$ laminated CFRP specimen is investigated. Also, a study on the evaluation of the stiffness degradation on the CFRP laminates is reported by Arikawa S. et al. (2017) where they observed the strain distribution of a CFRP laminate due to a light load measured by electronic speckle pattern interferometry (ESPI).

[DOI: 10.1299/mej.19-00003]

In this study, a digital image correlation (DIC) method is employed to measure the strain distribution at the macroscopic level during a tensile test to a cracked CFRP cross-ply laminate. Since it was first proposed in the 1980s, DIC is now extensively applied in many experimental mechanics researches (Yamaguchi I., 1981; Peters W.H. et al., 1982; Pan B. et al., 2009; Men Y., 2017). The advantage that DIC has over the standard method of using the strain gages is that the DIC approach is a non-contact strain measurement that can give out the displacement and strain distribution in loading, transverse and shear directions. Also, it gives point-by-point strain field, while the standard method only gives uniform strain (GOM ARAMIS HP, accessed date 2019.01.20). DIC application is not limited only for tensile loading but it can be also applied to a body under other types of loadings. DIC is also simple to use and cost effective compared to speckle interferometric and etc. (McCormick N. et al., 2010).

Therefore, the objective of this study is to measure the deformation around the damages in cross-ply CFRP laminates by using DIC system in various directions. For this purpose, thick CFRP $[0_4/90_{24}]_s$ and thinner $[0/90_6]_s$ laminates were tested. In laminates, usually a straight transverse crack will initially occur in off-axis plies followed by the following damages such as delamination, fiber fracture, and etc. To start, straight transverse cracks are induced in the laminates by using an artificial crack method. Then, X-ray radiography is used to detect the location of the straight cracks in order to be used for DIC observation to examine the strain distribution around the existed cracks. From the result, secondary mode damages of matrix cracking such as oblique and curved cracks also can be observed and are being discussed in this paper.

2. Experiment

2.1 Material

The materials used in this study and the properties of unidirectional materials are shown in Tables 1 and 2 respectively. Material properties of each material are obtained by conducting monotonic tensile test using Tensilon RTF-1350 A&D tensile test machine with cross head speed of 1mm/min. Strain gages are used to measure the average strain for this loading. The tensile loading is done to examine the fracture strength, fracture strain and stress/strain where cracks initially occur so that the suitable applied stress/strain range for DIC observation can be decided.

Table 1 Type of materials.

Raw material type	Prepreg (preimpregnated composite fiber)	
Resin system	T700SC/2592, Torayca	
Prepeg thickness (mm/ply)	0.15	
Laminate configuration	$[0_4/90_{24}]_s$	$[0/90_6]_s$
Laminate thickness (mm)	8.23	2.06

Table 2 Properties of unidirectional materials.

Young's modulus in 0^o direction E_1 [GPa]	123
Young's modulus in 90^o direction E_2 [GPa]	8.68
Shear modulus G_{12} [GPa]	3.92
Poisson's ratio ν_{12} [-]	0.33

The prepregs are stacked according to the stacking sequences shown in Table 1 and cured in an autoclave at a temperature of 130 degree Celsius and pressure of 0.2 MPa. Laminates are then cut into the measurement shown in Figure 2 by using a composite material cutting machine (AC-300CF, Maruto Testing Machine). In order to make sure matrix cracks uniformly occur on the specimen for easier damage observation by X-ray radiography and DIC system, the artificial crack method is induced in this study. This method is explicitly explained in Fikry et al. (2018) where artificial crack method can be done by making notches at both edges of the specimen by using a knife before pulling it in a tensile test machine with cross head speed of 1mm/min to a specific load. Then the specimen is unloaded back to zero and the notched edges are cut by using composite material cutting machine mentioned above at ±5mm from the edges.

[DOI: 10.1299/mej.19-00003]

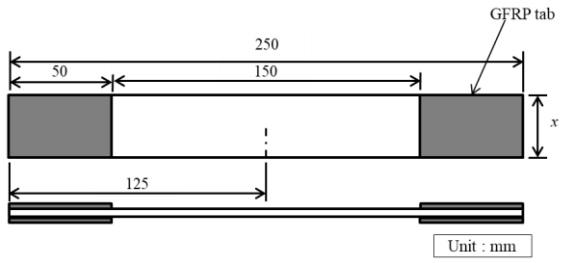

Fig. 2 Specimen's measurement.

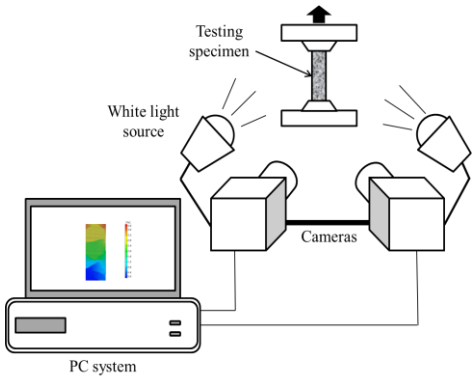

Fig. 3 Schematic figure of DIC setting.

2.2 Damage observation

After removing the notched edges, the specimens are then placed in X-ray radiography device (M-100S, SOFTEX) in order to detect the location of matrix cracks. Comparing the X-ray image with the specimen, the position of visible matrix transverse cracks is marked on the specimen. The DIC software and cameras used in this study is GOM ARAMIS system. ARAMIS is a non-contact optical deformation measuring system that analyzes, calculates and documents deformation occurring on the materials. ARAMIS recognizes the surface structure of the measuring object in digital camera images and allocates coordinates to the image pixels. The first image in the measuring project represents the undeformed state of the object. After or during the deformation of the measuring object, further images were recorded. Then, ARAMIS compares the digital images and calculates the displacement of the object characteristics.

Then, DIC apparatus is set up as shown in Figure 3 where tensile machine is different with the one used to obtain the mechanical properties of the laminates. The tensile test machine used in DIC observation is Shimadzu AG-X Plus and the cross head speed for this loading is maintained at 1mm/min. ARAMIS sensor unit is operated on a stand in order to optimally position the sensor with respect to the specimen. For the measurement setup, two cameras are used (stereo setup) that are calibrated prior to measuring. The specific cracks contained observation area in this study is about 20mm x 18mm so that the software measuring volume that has been selected is 35mm x 29mm. The suitable lens size for this measuring volume is 75mm with resolution of 2448 x 2050 pixels (Titanar 75mm, sensor used is ARAMIS 5M) while for calibration of the cameras, CQ1CP20 30X24 calibration panel is used. To facilitate the correlation, a stochastic pattern is applied to the specimen surface in order to provide a random grey-level a variation at the sufficient quality of which is fundamental to the precision of the measured displacement data. The stochastic pattern in this study was created by black and white color sprays where black spray was first applied as the fundamental while white sprays was carefully applied above the black surface. After creating the measuring project in the software, images are recorded in various load stages of the specimen where the frame frequency is 0.5Hz. When the area to be evaluated is defined and a start point is determined, the measuring project is computed. During computation, ARAMIS observes the deformation of the specimen through the images by means of various square or rectangular image details, called facets (In this study the facet size is 18 x 18 pixels which gives 0.45mm x 0.45mm). A homogenous field of displacements is assumed inside each facet. The value of strain was calculated by differentiate the distribution of displacement. Hence, it is difficult to obtain a smooth strain distribution. So, in order to reduce the effect of the displacement measurement error, the displacement distribution was functionally approximated by a least squares method in ARAMIS, and then the strain was calculated by differentiating the function. The gage length is 0.4mm where in order to ensure the required accuracy of the measurement of displacements on a body surface, the individual facets are overlap by 2 pixels. (GOM ARAMIS HP, accessed date 2019.01.20)

3. Results and Discussion

3.1 Monotonic tensile test

The mechanical properties such as Young's modulus, tensile strength, fracture strain and Poisson's ratio of each material used in study are shown in Table 3. Young's modulus was calculated for the strain range of 0.1-0.3%.

[DOI: 10.1299/mej.19-00003]

Table 3 Mechanical properties.

	Material	
	$[0_4/90_{24}]_s$	$[0/90_6]_s$
Young`s modulus [GPa]	24.1	24.5
Tensile strength [MPa]	373	326
Fracture longitudinal strain [%]	1.99	1.73
Poisson`s ratio	0.05	0.03

From the stress-strain curve of both laminates shown in Figure 4, we can see that both laminates showing almost similar properties where there are no significant changes due to multiplication of the laminates thickness when the ratio of 0 degree ply towards 90 degree ply is maintained. The main objective of doing this test is to examine the stress/strain where initial crack started to form in 90 degree ply. This result then becomes our reference for the artificial crack method because a specific tensile stress value can be decided for the loading in order to create the artificial cracks. From the result of both laminates, initial cracks started to form at about the same strain and stress which are 0.5% and 125MPa respectively. This can be determined by observing the nonlinearity of the curve. The strain value is measured by 2mm strain gages pasted at the center and on both sides of the specimen. The nonlinearity of the stress-strain curve is due to the occurrence of matrix cracks in the strain gage range. The nonlinearity of the stress-strain curve of $[0_4/90_{24}]_s$ laminate can be observed clearly after the strain of 0.5% showing that the cracks formed in this laminate have large effects on the nonlinearity of the curve. On the other hand, the nonlinearity of the curve for $[0/90_6]_s$ laminate are not so obvious showing that the cracks formed in this laminate have a smaller effect on it. This phenomenon may be due to the thickness of the off axis ply. Based on the formation of cracks in the strain gage range, those cracks occurring in thicker laminates contribute to a larger jump of the strain value compared to in thinner laminates. Also, the nonlinearity of stress-strain curve of $[0_4/90_{24}]_s$ laminate can be observed at an earlier stage (strain of 0.5-1.2%) and then become less as strain increases. This showed that for thicker laminates, the cracks formation rate is higher at the earlier stage, but become lower when the strain is further increased. On the other hand, in $[0/90_6]_s$ laminate, inlinearity of the curve occurred gradually after the strain of 0.5% (initial crack).This may happen because in thinner laminates, cracks density gradually increases as the strain increases.

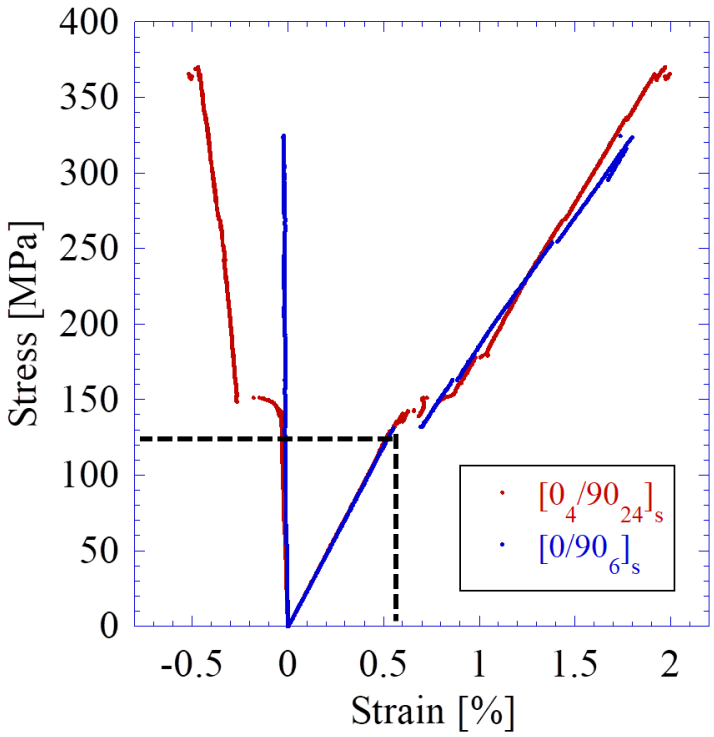

Fig. 4 Stress-strain curve of monotonic tensile test.

[DOI: 10.1299/mej.19-00003]

3.2 DIC damage observation

Figure 5 shows the transverse cracks observed by X-ray radiography. This cracked laminate is then loaded again for the DIC deformation measurement. One part of the laminate with three existed adjacent transverse cracks (Fig. 6(a)) is selected and the DIC strain distribution result for the selected area is shown in Figure 6(b & c). Figure 6(d) shows the plotted average strain distribution towards the specimen length. The direction ***y*** in the figure indicates the loading direction, ***x*** is width (straight transverse cracks) direction while ***z*** is the thickness direction of the specimen.

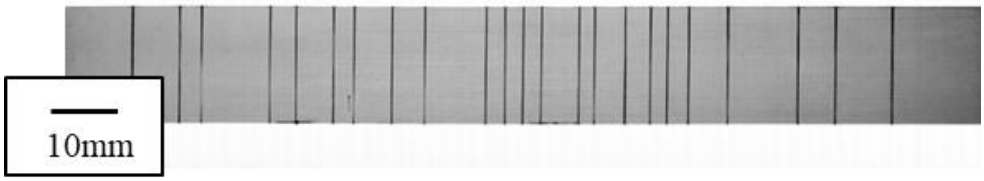

Fig. 5 X-ray radiography from surface direction of $[0/90_6]_s$ laminate.

The tensile stress for this observation is set to 180MPa where cracks appeared clearly by the DIC color scale of strain distribution. As shown in Figure 6(b & c), the strain values are higher at the cracks area with average strain of 0.9% compared to area with no cracks which is about 0.62%. However, when the average strain distribution is plotted such in Figure 6(d), we can observe a phenomenon where the strain values are dispersed and at the center of the crack area, the strain values dropped. This can be observed clearly by the red arrows showing in the figure. This is a normal phenomenon when DIC observation is done from the surface of the specimen especially for laminates that have 0 degree ply as outer ply where cracks occurred only in the off-axis ply. In this case, matrix transverse cracks occurred in 90 degree ply and the DIC observation is done from the surface of the 0 degree ply. The stress distribution around the cracks area inside the laminates due to the occurrence of the matrix cracks caused the strain distribution to become dispersed and cause the strain value at the center of the cracks to drop as in Figure 6(d).

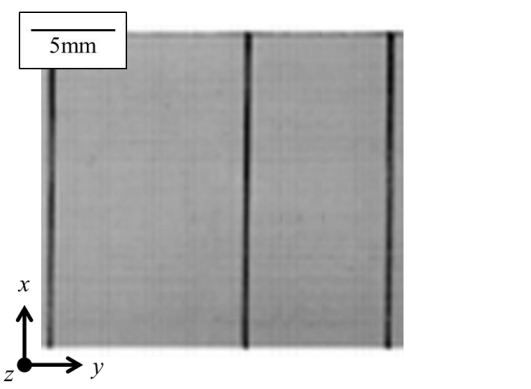

a. X-ray radiograph of transverse cracks in laminate

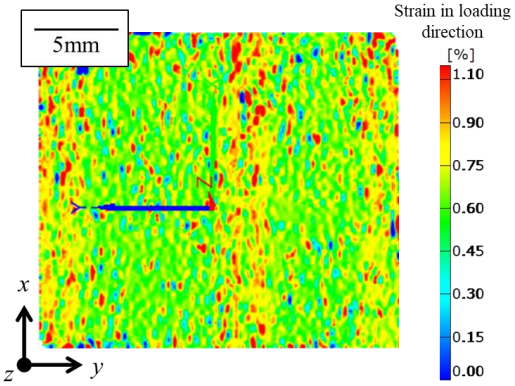

b. DIC strain distribution in loading direction

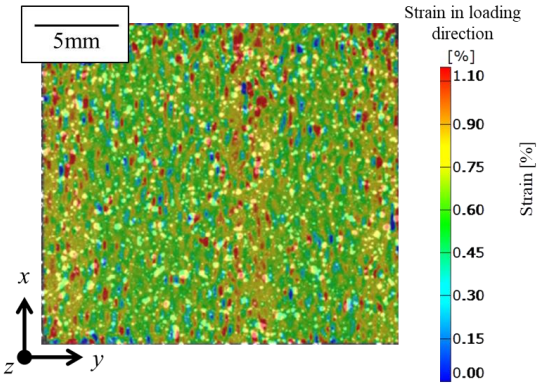

c. DIC strain distribution in loading direction (with random pattern)

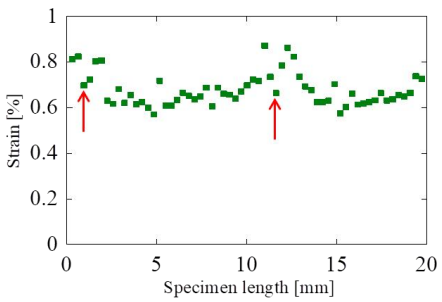

d. Plotted DIC strain distribution

Fig. 6 Crack observation from surface direction of $[0/90_6]_s$ laminate by X-ray radiography and DIC.

[DOI: 10.1299/mej.19-00003]

3.3 Secondary mode damages of matrix cracks

Other than making DIC observation from the surface of the laminates, we also made a DIC strain observation from the thickness direction of the laminates. Unfortunately, due to the limitation of our DIC system to detect a very small measuring area which is the edge surface area of the $[0/90_6]_s$ laminate (with thickness of 2mm), we did only DIC strain observation from the thickness direction of thicker $[0_4/90_{24}]_s$ laminate with the edge thickness of about 8mm.

Figure 7 shows the DIC observation from the thickness direction of $[0_4/90_{24}]_s$ laminate where (a) is the displacement distribution, (b) and (c) is the strain distributions and (d) is the plotted strain distribution taken at the cutting line shown in the figure. This figure shows that the cracks formed in 90 degree ply of the laminate are not only straight transverse cracks but also some other cracks called secondary mode damages. In this figure we can see three distinctly different types of matrix cracks which are straight transverse cracks, oblique (partial angled) cracks and curved cracks. Curved crack is a matrix crack that initially forms as partial angled crack extending from the ply interface oriented at an angle less than 90 degree while oblique crack is a crack that forms incompletely through the off-axis ply near a straight crack. These cracks can be observed near a straight crack and grow toward the straight crack. There are also occurrences of two curved or oblique cracks located on one side of a straight crack.

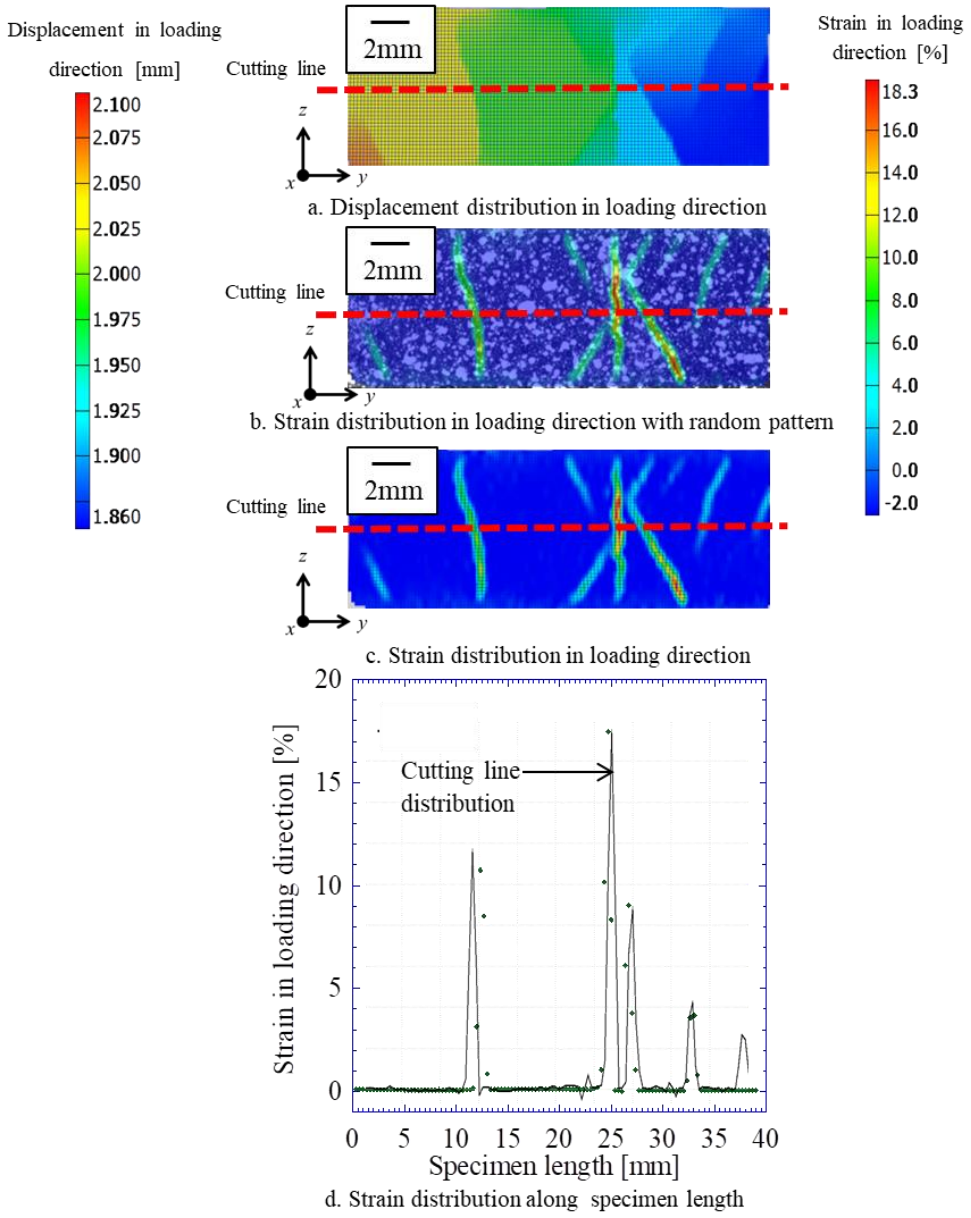

Fig. 7 DIC observation from the thickness direction of $[0_4/90_{24}]_s$ laminate.

[DOI: 10.1299/mej.19-00003]

However, we can also observe a large strain appears at the matrix cracks where this is actually considered as a demerit of the optical-displacement-deformation measuring method including DIC because this phenomenon is actually caused by the error during the strain calculation from the displacement value captured by DIC. The actual strain on the elastic cracks surface should be zero due to the stress free state. This virtual large strain appears when the gage length for the strain calculation from the displacement result is larger than the matrix crack's opening displacement. Despite having this demerit, DIC however does show clearly the occurrence of the secondary mode damages in the laminates which is very useful information in order to evaluate the matrix cracks propagation in the laminates. We then used X-ray radiography again to observe from the surface direction of the $[0_4/90_{24}]_s$ laminate after the occurrence of these cracks. The result is shown in Figure 8 where the image clearly shows different kinds of cracks characteristics. In this figure, the straight cracks appear as a sharp narrow band while for curved cracks, it appears as a wider and fuzzy band. A similar observation is reported in Groves (1986).

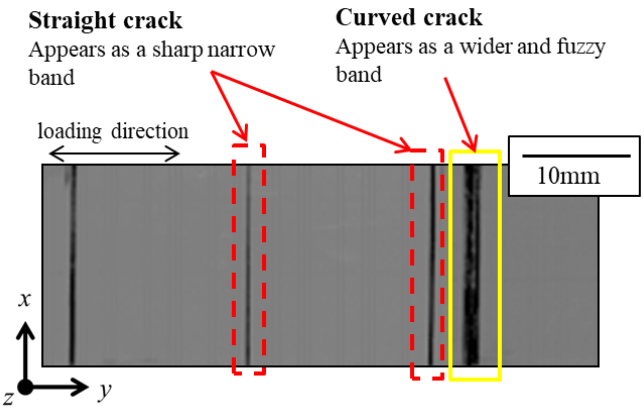

Fig. 8 X-ray radiography from surface direction of $[0_4/90_{24}]_s$ laminate.

In order to explain the occurrence of these secondary mode damages, we observed the DIC shear strain distribution from the thickness direction of the $[0_4/90_{24}]_s$ laminate. Figure 9 shows the DIC strain in loading direction and shear strain distribution observation at earlier stages where oblique and curved cracks have not yet occurred in this laminate. As shown in Figure 9(b), shear strain in the red circles marked as '***k***' at the upper left and the lower right area near the straight crack is larger than the shear strain of other non-cracked area on the laminate. On the other hand, at the upper right and lower left area around the cracks highlighted with red circles marked as '***j***' showing a larger negative shear strain where this is a normal phenomenon where the shear strain value can be positive or negative value due to the symmetrical properties of matrix cracks in laminates.

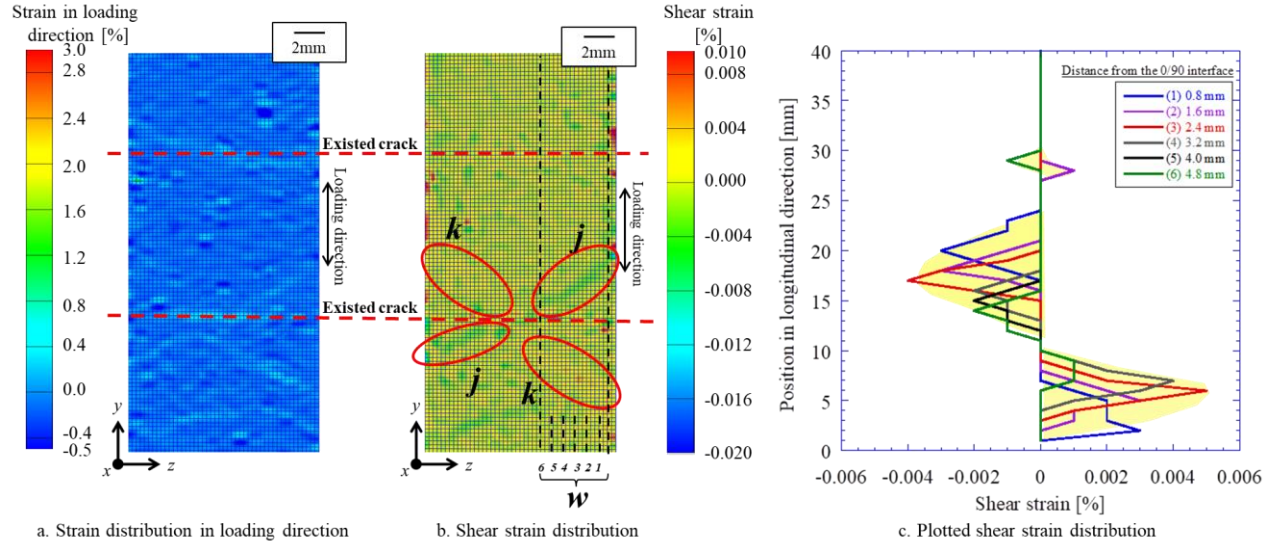

Fig. 9 Strain distributions around the existed cracks before the formation of secondary mode damages of matrix cracking from the thickness direction of the specimen.

[DOI: 10.1299/mej.19-00003]

This can be observed clearly also in Figure 9(c) where shear strain in straight lines along the specimen length labelled as 1-6 in ***w*** area in Figure 9(b) is plotted against the specimen length. The area highlighted in yellow in this graph is the average shear strain value based on the shear strain at each point. From this relationship, we can observe the points where shear strain are highest and with the possibility of the initiation of the oblique cracks. This is then confirmed by comparing this figure to Figure 7(b) and (c), where the location of oblique cracks is exactly at the points with the highest shear strain. The larger distribution of shear strain in this area shows that this area has high accumulation of maximum principle stress. This may be the reason that caused the initiation of the oblique cracks seen in Figure 7(b) and (c). While for curved cracks, we can conclude that when two oblique cracks propagated from opposite side of each other, they meet and combine to become a curved shape near to the existed straight crack. Oblique cracks and curved cracks found on the fractured specimen are then observed by microscope (KEYENCE VHX-2000) for clearer observation from the thickness direction of the specimen (Figure 10).

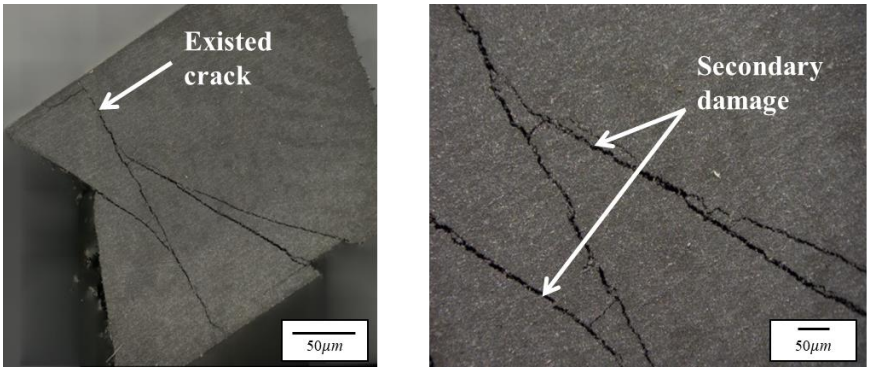

Fig. 10 Microscopic specimen's edge observation of $[0_4/90_{24}]_s$ laminate.

FE analyses of oblique cracking by Jalalvand et al. (2014) providing supporting evidence for the postulated growth mechanism such like in the result of this study. They examined the stress distribution around the straight transverse crack. From the result of the distribution of maximum principal stress in the 90 degree ply, they reported that principal stress is higher at the areas around the interface near to the existed straight cracks. This suggests that if a crack initiates from the area with high values of maximum principal stress, the crack would propagate in an oblique manner towards the closer transverse crack. The DIC observation of oblique cracks in this study is in a good agreement with the result in this analysis.

4. Conclusion

The deformation measurement around damages in CFRP cross-ply laminates is experimentally investigated by using DIC in this study. The crack can be clearly indicated by the DIC strain distribution where the strain values are higher at the cracks area compared to area with no cracks. We found a phenomenon where the strain values are dispersed at the crack area. The occurrence of matrix cracking in secondary mode damages such as oblique and curved cracks is a possible reason for this phenomenon. Usually, the straight crack is formed first followed by oblique cracks and curved cracks that occur close to existing straight cracks. The orientation and location of the oblique and curved cracks corresponded to the orientation of the principal stresses in the vicinity of a straight crack and this is proved by the DIC deformation observation and previous analysis study. These types of matrix cracks may also contribute to degradation of laminate's mechanical properties such as stiffness reduction and etc. From this study we can conclude that DIC method can be applied for the deformation measurement of any material from any direction including the shear direction and etc. This method will be used efficiently in our future works in order to study about the damages especially in composite materials.

Acknowledgement

We would like to show our sincere gratitude to Professor Nobuo Takeda at Japan Aerospace Exploration Agency (JAXA) and Professor Shu Minakuchi at Graduate School of Frontier Sciences, The University of Tokyo for allowing us to use their laboratory facilities (DIC-ARAMIS and tensile test machine) during this research. Special thanks of

[DOI: 10.1299/mej.19-00003]

gratitude to MARA Education Foundation (YPM) for sponsoring the corresponding author to study in Japan in order to complete this research study.

References

Arikawa S., Endo Y., Evaluation of Stiffness Degradation on CFRP Laminate by Measuring Strain Distribution Using Speckle Interferometry, Journal of the Japanese Society for Experimental Mechanics, Vol. 17, No 1 (2017), pp.15-20.

Boniface L., Smith P., Bader M., Rezaifard A., Transverse ply cracking in cross-ply CFRP laminates – Initiation or propagation controlled?, Journal of Composite Materials, Vol. 31, (1997), pp.1080-1112.

Fikry M., Ogihara S., Vinogradov V., The effect of matrix cracking on mechanical properties in FRP laminates, Mechanics of Advanced Materials and Modern Processes, Vol. 4, (2018) No 3.

GOM ARAMIS Homepage, https://www.gom.com/3d-software/gom-correlate.html, Accessed date: 2019.01.20.

Groves S., Harris C., Highsmith A., Allen D. and Norvell R., An Experimental and Analytical Treatment of Matrix Cracking in Cross-Ply Laminates, Experimental Mechanics, Vol. 27, No 1 (1987), pp.73-79.

Han Y., Hahn H., A simplified analysis of transverse ply cracking in cross-ply laminates, Compos Sci Technol, Vol. 31, (1988), pp.165-177.

Hashin Z.,Analysis of cracked laminates: a variational approach, Mech Mater, Vol. 4, No 2 (1985), pp.121–36.

Hosoi A., Sato N., Kusumoto Y., Fujiwara K., Kawada H., High-cycle fatigue characteristics of quasi-isotropic CFRP laminates over 10^8 cycles (initiation and propagation of delamination considering interaction with transverse cracks), International Journal of Fatigue, Vol. 32 (2010), pp.29-36.

Hu S., Bark J., Nairn J., On the phenomenon of curved microcracks in $[(S)/90_n]_s$ laminates: their shapes, initiation angles and locations. Composites Science and Technology, Vol. 47, No 4 (1993), pp.321–9.

Jalalvand M., Wisnom M., Hosseini H., Mohammadi B., Experimental and numerical study of oblique transverse cracking in cross-ply laminates under tension, Composites: Part A Vol. 67 (2014) pp.140–148.

Lim S., Hong C., Prediction of transverse cracking and stiffness reduction in cross-ply laminated composites, Journal of Composite Materials, Vol. 23, (1989), pp.695-713.

McCormick N., Lord J., Digital Image Correlation, Materials today, Vol. 13, No 12 (2010), pp.52-54.

Men Y., Li X., Chen L., and Fu H., Experimental study on the mechanical properties of porcine cartilage with microdefect under rolling load, Journal of Healthcare Engineering, Vol. 2017 (2017).

Ogihara S., Takeda N., Interaction between transverse cracks and delamination during damage progress in CFRP cross-ply laminates. Composites Science and Technology, Vol. 54, No 4 (1995), pp.395–404.

Pan B., Qian K., Xie H., and Asundi A., Two-dimensional digital image correlation for in-plane displacement and strain measurement: a review, Measurement Science and Technology, Vol. 20, No. 6 (2009).

Parvizi A., Garrett K., Bailey J., Constrained cracking in glass fibre-reinforced epoxy cross-ply laminates, Journal of Material Science, Vol. 13, (1978), pp.195-201.

Peters W. and Ranson W., Digital imaging techniques in experimental stress analysis, Optical Engineering, Vol. 21, No. 3 (1982).

Praveen G., Reddy J., Transverse matrix cracks in cross-ply laminates: stress transfer, stiffness reduction and crack opening profiles, Acta Mechanica, Vol. 130, (1998), pp.227-248.

Vinogradov V., Analysis of initial accumulation of matrix cracks in angle-ply laminates, Proceedings of 20th International Conference on Composite Materials (ICCM20) (2015).

Vinogradov V., Hashin Z., Variational analysis of cracked angle-ply laminates, Composites Science and Technology, Vol. 70, No 4 (2010), pp.638–646.

Wang Q., Ri S., Tsuda H., Takashita Y., Kitamura R., Ogihara S., Materials (Basel), Vol. 11, No 9 (2018).

Xia Z., Carr R., Hutchinson J., Transverse cracking in fiber-reinforced brittle matrix, cross-ply laminates, Acta Metall Mater, Vol. 41, (1993), pp.2365-2376.

Yamaguchi I., A laser-speckle strain gage, Journal of Physics E: Scientific Instruments, Vol. 14, No. 11 (1981), pp.1270–1273.

Zhang J., Fan J., Soutis C., Analysis of multiple matrix cracking in $[\pm\theta_m/90_n]_s$ composite laminates. Part 2: development of transverse ply cracks, Composites, Vol. 23 (1992), pp.299-304.

[DOI: 10.1299/mej.19-00003]